

## Monomer Environments during the Solid-State Photodimerization of *trans*-*p*-Bromocinnamic Acid

Zeev Savion and David L. Wernick\*<sup>1</sup>

School of Chemistry, Raymond and Beverly Sackler Faculty of Exact Sciences, Tel Aviv University, Ramat Aviv 69978, Israel

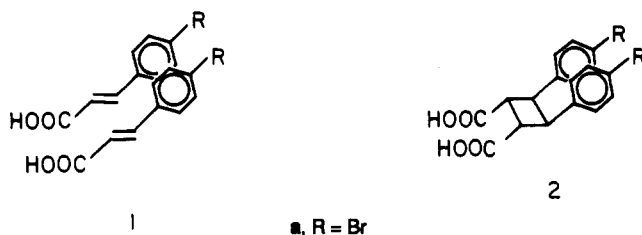
Received October 28, 1992

The photodimerization of *trans*-*p*-bromocinnamic acid, possessing a stack crystal structure in which each monomer has two monomeric nearest neighbors in the stack dimension, was monitored by FTIR spectroscopy. Upon UV irradiation, FTIR spectral shifts and transient absorptions indicated that residual monomers were present in altered crystal-structure environments. The results are interpreted according to a kinetic model in which monomers have one or two dimeric nearest neighbors at intermediate levels of photoconversion.

The kinetics of crystalline-state organic reactions are complex because the environment of reactant molecules changes substantially during the course of reaction. Each reactant molecule is initially surrounded solely by other reactants. At intermediate conversions, many reactants are partially or entirely surrounded by product molecules. In addition, the geometry of reactant-reactant interactions may change as the crystal lattice adapts to accommodate the product molecules.

In this paper, we report direct observation of such environmental changes by FTIR spectroscopy.

A few years ago, we proposed<sup>2</sup> an idealized kinetic model of environmental changes in the photodimerization of conjugated alkenes in "stack"- or "β"-type crystal structures.<sup>3,4</sup> This reaction is exemplified by the photodimerization of certain cinnamic acids **1**, yielding β-truxinic acids **2**.



The model assumes three main environments for **1**, as illustrated in Figure 1. These are termed "two-sided", "one-sided", and "isolated" environments, according to the number of monomeric nearest neighbors that each monomer possesses in the stack dimension with which it can potentially react.

According to this model, the concentration of two-sided monomers decreases monotonically during the course of photoreaction (Figure 2). In contrast, the concentration of one-sided monomers passes through a maximum of about 22% with respect to the total number of starting

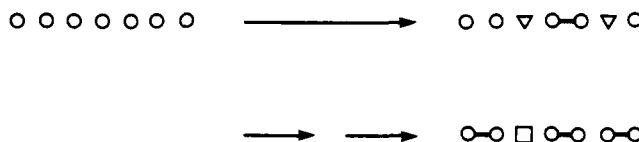


**Figure 1.** Idealized photodimerization model. Dimers (o-o) are formed with uniform probability among pairs of neighboring monomers along an infinite, one-dimensional stack. As dimerization proceeds, some two-sided monomers (having two monomeric neighbors with which it can potentially react, O), are blocked off and become one-sided (▽) or isolated (□).

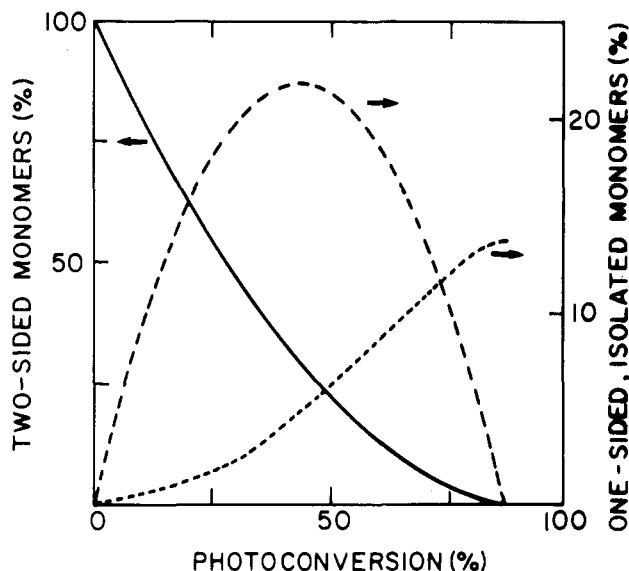


**Figure 2.** Concentration of two-sided (—), one-sided (---), and isolated (···) monomers in the idealized model.

monomers. The concentration of isolated monomers (which cannot react) increases slowly to a final value of  $1/e^2 = 13.5\%$ . The theoretical maximum yield of the reaction is thus  $1 - 1/e^2 = 86.5\%$ .

Experimentally, the yield of photodimerizations in stack crystal structures is generally limited to  $\leq 90\%$ , in agreement with this model. Fluorescence from proposed isolated monomers has been detected in photodimerizations of anthracene, butadiene, and stilbene derivatives.<sup>5</sup>

(1) Present address: TIRZA, P.O. Box 443, Elkana, D. N. Efrain 44814, Israel.

(2) Wernick, D. L.; Schochet, S. *J. Phys. Chem.* **1988**, *92*, 6773-8. See also: Harris, K. D. M.; Thomas, J. M.; Williams, D. *J. Chem. Soc., Faraday Trans.* **1991**, *87*, 325-31.

(3) (a) Cohen, M. D.; Schmidt, G. M. J.; Sonntag, F. I. *J. Chem. Soc.* **1964**, 2000-13. (b) Schmidt, G. M. J. *J. Chem. Soc.* **1964**, 2014-21.

(4) Reviews: (a) Green, B. S.; Arad-Yellin, R.; Cohen, M. D. In *Topics in Stereochemistry*; Eliel, E. L., Wilen, S. H., Allinger, N. L., Eds.; Wiley: New York, 1986; Vol. 16, pp 131-217. (b) Cohen, M. D. *Tetrahedron* **1987**, *43*, 1211-24. (c) Cohen, M. D. *Angew. Chem., Int. Ed. Engl.* **1975**, *14*, 386-93.

(5) (a) Ebeid, E.; Morsi, S.; Williams, J. O. *J. Chem. Soc., Faraday Trans. 1* **1979**, *75*, 1111-9. (b) Cohen, M. D.; Elgavi, A.; Green, B. S.; Ludmer, Z.; Schmidt, G. M. J. *J. Am. Chem. Soc.* **1972**, *94*, 6776-9. (c) Cohen, R.; Ludmer, Z.; Yakhot, V. *Chem. Phys. Lett.* **1975**, *34*, 271-4.

Recently, unimolecular byproducts in the solid-state photodimerization of an azadiene were proposed to be formed from isolated and one-sided monomers, in semi-quantitative agreement with a kinetic model.<sup>6</sup>

We now report that discrete monomer environments—tentatively identified with the one-sided and isolated environments of the idealized model—can be observed directly by FTIR during the photodimerization of *trans*-*p*-bromocinnamic acid **1a**.

### Experimental Methods

**1a** was purchased from Aldrich Chemical Co. and recrystallized from aqueous ethanol before use. Infrared spectra were determined with a Nicolet 5DX FTIR spectrometer; typically, 300 scans were accumulated.

Samples were prepared as follows: A thin layer of **1a** was crystallized by slow evaporation of a 1.1 wt % acetone solution on a homemade 13-mm KBr window. The layer thickness was  $\approx 7 \mu\text{m}$  (containing  $\approx 1 \text{ mg}$  of **1a**), permitting both FTIR and UV examination of the same sample. The maximum IR absorbance was low ( $\leq 0.2 \text{ A}$ ), so that spectroscopic nonlinearities due to nonuniform layer thickness ("wedging") could be neglected.<sup>7</sup> The layer was polycrystalline, with crystallites randomly oriented in a plane parallel to the window surface (polarizing microscopy). The crystallites were nonrandomly oriented with respect to an axis perpendicular to the window surface (inferred from the dependence of the IR spectrum on the angle between the window and the IR beam). No change in the microscopic appearance of the layer was detectable during reaction.

Each kinetic run was conducted on a single thin-layer sample. The sample was mounted in a holder and irradiated at 300 or 350 nm (32 8-W Sylvania F8P5/CW or F8P5/BLB8W phosphor-coated mercury lamps mounted in a Rayonet RPR-100 photoreactor) at ambient temperature. The UV absorbance of the sample at these wavelengths was  $< 0.05$ , ensuring uniform irradiation throughout the layer thickness. At intervals, the sample was briefly removed from the photoreactor for FTIR or UV examination. At low levels of conversion, the FTIR spectra were stable upon storage of the samples in the dark for periods of up to 21 days. At high conversions, small spectral changes were observed upon storage in the dark for 2–3 days, probably due to slow recrystallization of the product phase.<sup>4a,b</sup>

During the course of each kinetic run, conversion was estimated in situ from the FTIR absorbance at  $984 \text{ cm}^{-1}$ . This absorbance was calibrated ( $\pm 10\%$ ) by comparison with independent samples, in which conversion was established by dissolving the sample in  $\text{CD}_3\text{COOD}$  and  $^1\text{H-NMR}$  integration. Calibration of the integrated intensity at  $963\text{--}992 \text{ cm}^{-1}$  was also employed for this purpose and gave equivalent results.

### Results

Thin-layer samples of polycrystalline **1a** were irradiated at 300 or 350 nm. During irradiation, UV absorbance at  $\lambda_{\text{max}} = 276 \text{ nm}$  decreased monotonically (Figure 3). The UV absorbance was not useful for quantitative kinetic measurements, however, because of strong light scattering by the sample. The photoproduct scraped from the window surface was identical to authentic<sup>3,9</sup> **2a** mixed with a small amount of residual **1a** by  $^1\text{H-NMR}$  ( $\text{CD}_3\text{COOD}$  solution) and FTIR (KBr pellet) spectroscopy. Authentic **2a** was stable under our conditions of irradiation.

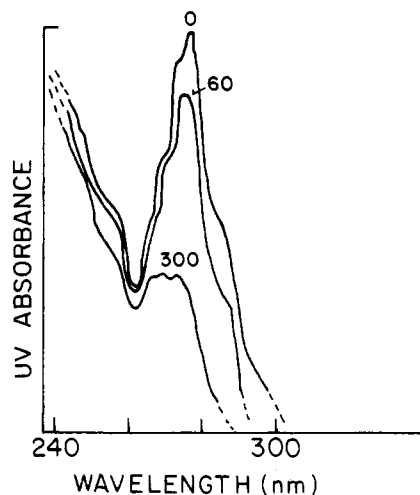


Figure 3. UV spectra of **1a** (thin layer), after the indicated times (min) of 300-nm irradiation. The base line is sloped due to light scattering by the solid samples.

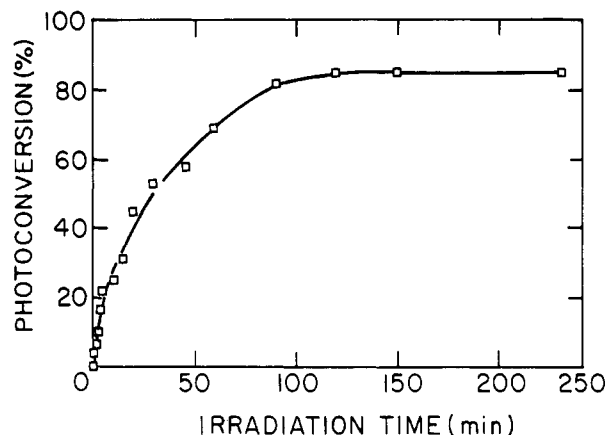


Figure 4. Kinetics of photodimerization of a typical sample at 300 nm.

The reaction yield was measured at long irradiation times (up to 840 min) by scraping the product from the KBr window and integration of its solution-phase  $^1\text{H-NMR}$  spectrum. The yield was  $90 \pm 5\%$  measured by this method (precision limited by the small quantity of material ( $\approx 1 \text{ mg}$ ) in the thin-layer samples).

A typical kinetic plot, determined by NMR calibration of the  $984\text{-cm}^{-1}$  FTIR band of **1a**, is shown in Figure 4. The reaction rate varied considerably among numerous tested samples, and the rate was slower under 350-nm irradiation than at 300 nm. However, the qualitative changes in the FTIR spectra described below were reproducible among the samples under all tested conditions.

As expected, the conjugated carbonyl stretching absorption of **1a** ( $1668\text{--}1676 \text{ cm}^{-1}$ ) shifted during the photoreaction to the unconjugated absorption of **2a** ( $1700\text{--}1711 \text{ cm}^{-1}$ ), and the olefinic stretching absorption ( $1624 \text{ cm}^{-1}$ ) essentially disappeared (Figure 5a).

The olefinic out-of-plane deformation band of **1a** ( $984 \text{ cm}^{-1}$ )<sup>10</sup> diminished and shifted to lower energies with increasing photoconversion. At intermediate levels of photoconversion ( $\approx 10\text{--}50\%$ ), this band was observed at

(6) Teng, M.; Lauher, J. W.; Fowler, F. W. *J. Org. Chem.* 1991, 56, 6840–5.

(7) Hirshfeld, T. In *Fourier Transform Infrared Spectroscopy*; Ferraro, J. R., Basile L. J., Eds.; Academic Press: London, 1979; Vol. 2, pp 215–21.

(8) (a) Osaki, K.; Schmidt, G. M. *J. Isr. J. Chem.* 1972, 10, 189–93. (b) Nakanishi, F.; Nakanishi, H.; Tsuchiya, M. *Bull. Chem. Soc. Jpn.* 1976, 49, 3096–9.

(9) Further identified by derivatization to the anhydride.

(10) Bellamy, L. J. *The Infrared Spectra of Complex Molecules*; Wiley: New York, 1959.

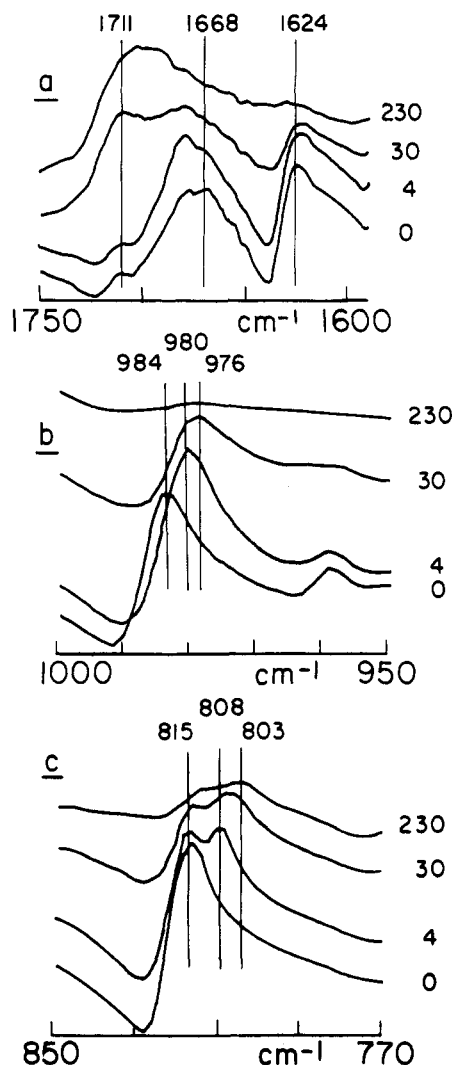


**Figure 5.** Changes in FTIR spectrum after 0, 4, 30, and 230 min of irradiation at 300 nm (photoconversions ca. 0, 10, 50, and 85%, respectively): (a) carbonyl and olefin stretching; (b) olefin out-of-plane deformation; (c) aromatic CH out-of-plane deformation.

980  $\text{cm}^{-1}$  (Figure 5b). At the conclusion of reaction, a weak absorption remained at 976  $\text{cm}^{-1}$ .

Striking behavior was exhibited by the aromatic CH out-of-plane deformation band of **1a** (816  $\text{cm}^{-1}$ ).<sup>10</sup> This band diminished rapidly at 10–50% conversion and was supplemented by a new, discrete band at 808  $\text{cm}^{-1}$  with a maximum intensity of about 20% of that of the starting 816  $\text{cm}^{-1}$  band (Figure 5c). At higher conversions (>50%), both the 816 and 808  $\text{cm}^{-1}$  bands diminished roughly in parallel and were replaced by a weak absorption at 803  $\text{cm}^{-1}$ .

Absorbances at several frequencies varied nonmonotonically with increasing conversion. This was the case for absorbances at 1668 (carbonyl stretching), 1624 (olefinic stretching), 1302 (olefinic in-plane deformation), and 546  $\text{cm}^{-1}$  (unassigned), each of which increased slightly at low conversions (up to  $\approx 20\%$ ) and decreased at higher conversions. Absorbances at many other frequencies varied monotonically.

### Discussion

Schmidt et al.<sup>3</sup> reported that **1a** crystallizes in the stack structure and gives the  $\beta$ -truxinic acid **2a** cleanly upon

irradiation. In our thin-layer crystalline samples, the reaction proceeded with a  $90 \pm 5\%$  product yield, in agreement with Schmidt's reported 90% yield and with the theoretical yield of 86.5% predicted by the idealized model.

The spectroscopic results suggest the development of two new monomer environments during the course of photodimerization, in addition to the starting two-sided environment. Evidence for the existence and nature of these environments is discussed below.

**One-Sided Environment.** The photodimerization of **1a** is believed to be a concerted  $2\pi + 2\pi$  process; no intermediate involving covalent bonds between two molecules of **1a** is expected along the reaction pathway.

The FTIR spectra show several anomalies, however, which indicate the presence of a transient olefinic species at high concentrations in the crystal lattice. These anomalies include a shift in absorption frequency of the olefin out-of-plane deformation mode (Figure 5b); a discrete, transient absorption in the aromatic out-of-plane deformation region (Figure 5c); and nonmonotonic absorbance variation in several other bands characteristic of **1a**. All of these anomalies persisted at photoconversions of 20–50% and disappeared upon further irradiation of the sample. The FTIR spectra remained unchanged, however, upon storage of the samples for several days in the dark, demonstrating that the anomalies are due to a thermally stable species.

These observations are consistent with an intermediate comprising a molecule of **1a** interacting with monomeric and/or dimeric neighbors within an altered crystal structure environment, formed at intermediate levels of photoconversion.

In accordance with the kinetic model described in the introduction, we suggest that this intermediate environment is the "one-sided" environment of the idealized dimerization model (Figure 1), in which the monomer interacts with one monomeric and one dimeric nearest neighbor in the stack dimension.

Consistent with this interpretation, anomalous spectral shifts occurred in vibrational modes oriented in the stack ("out-of-plane")<sup>3b</sup> dimension. The observation that these shifts were in the direction of lower vibrational energies suggests that repulsive interactions between **1a** and its nearest neighbors in the stack dimension may be reduced in the one-sided environment.

An effect of this type can be rationalized by crystal lattice distortions that inevitably occur upon dimerization<sup>11</sup> (Figure 6). Thus, the van der Waals distance of 3.97 Å between neighboring monomers<sup>3b</sup> is reduced to a covalent distance of  $\approx 1.54$  Å in the dimer. This contraction pulls the cyclobutane moiety of the dimer away from its monomeric nearest neighbors in the stack (which are present in one-sided or isolated environments). At the same time, the aromatic and carboxy substituents of **1a** swing out of the olefinic plane as the dimer is formed. These geometric changes are expected to alter the repulsive interactions in the stack dimension.

The maximum intensity of the 808  $\text{cm}^{-1}$  absorption was  $\approx 20\%$  of the starting intensity at 816  $\text{cm}^{-1}$ . Although the extinction coefficients of these bands are unknown, this is qualitatively consistent with the theoretical maximum

(11) (a) Desiraju, G. R.; Kannan, V. *Proc. Ind. Acad. Sci. (Chem. Sci.)* 1986, 96, 351–62. (b) McBride, J. M.; Segmuller, B. E.; Hollingsworth, M. D.; Mills, D. E.; Weber, B. A. *Science* 1986, 234, 830–35.

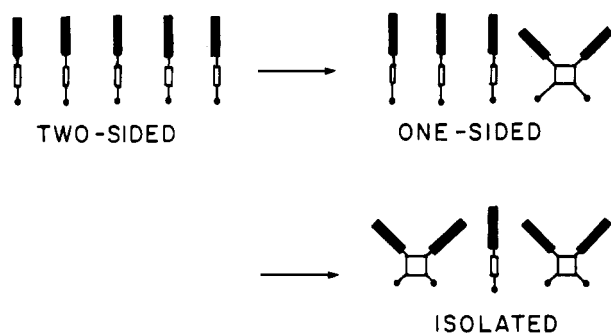


**Figure 6.** Interactions between a monomer and its nearest neighbors in the stack dimension are altered in the one-sided and isolated environments.

concentration of monomers in the isolated environment (22%, Figure 2) predicted by the idealized model. All of the transient anomalies were observed at ca. 20–50% photoconversion, consistent with the range of conversions at which a high concentration of one-sided monomers is expected (Figure 2).

**Isolated Environment.** The dimerization yield in stack crystal structures is limited by the formation of isolated monomers (Figure 1).<sup>2,3</sup> The observed photo-

dimerization yield of **2a** was  $90 \pm 5\%$ , even after prolonged irradiation. The yield was not limited by any side reaction, and the recovered photoproduct **2a** was mixed only with residual starting material. The observed yield agrees with the value of 90% reported by Cohen and Schmidt<sup>3a</sup> and is close to the theoretical value of 86.5% predicted by the idealized model.<sup>2</sup> Thus, it appears that  $\approx 10\%$  of the starting **1a** monomers remain present at the conclusion of reaction, presumably in the isolated environment.

In support of this conclusion, a weak olefinic absorption at  $976\text{ cm}^{-1}$  was observed at the end of reaction (Figure 5b). This absorption, as well as a weak residual aromatic absorption at  $803\text{ cm}^{-1}$  (Figure 5c), can probably be assigned to **1a** in the isolated environment. If these assignments are correct, the shift to lower vibrational energies relative to the one-sided environment ( $980$  and  $808\text{ cm}^{-1}$ , respectively) can be explained as a further reduction in out-of-plane nearest neighbor interactions, as suggested above (Figure 6).

**Acknowledgment.** The authors are indebted to Prof. Ben Zion Fuchs for the use of photochemical equipment and for helpful discussions and to Joseph Levy for preparing the KBr windows.